Experimental Investigation of the Flexural Behavior of Geopolymer Concrete Beams with Different Reinforcement Schemes

Nadia O. Nofal [1], Hossam H. Ahmed [2], Gehan A. Hamdy [2], Ali S. Shanour [2] , Salma G. Saad [2],*

[1] *Housing and Building National Research Centre, Giza, Egypt*
[2] *Department of Civil Engineering, Faculty of Engineering at Shoubra, Benha University.*
Corresponding author

E-mail address: nadia_nofal@yahoo.com , hossam@heliopolis-hctc.com , gehan.hamdy@feng.bu.edu.eg , ali.shnor@feng.bu.edu.eg ,salmagamal022@gmail.com

Abstract: This paper presents an experimental study of the flexural behavior of geopolymer concrete beams reinforced with steel and Glass Fiber-Reinforced Polymers (GFRP) bars in addition to two types of fibers in the mixture: steel fibers and polypropylene fibers. Ten beams divided into three groups were cast and experimentally tested under four-point bending up to failure. Mid-span deflection, strain at reinforcement bars, and crack pattern of the examined beams were recorded and analyzed. The results showed that the crack width and deflection at failure were notably reduced by increasing the reinforcement ratio of GFRP bars and steel bars. Reinforced geopolymer concrete beams showed enhancement of flexural capacity than normal reinforced concrete beams. Geopolymer concrete beams reinforced with steel bars achieved increment for ultimate load and corresponding deflection by 8.78%, and 114.66% respectively than normal concrete beams. In addition, the ultimate load and deflection of geopolymer concrete beams reinforced by glass fiber polymer bars showed an increase of 1.54%, and 25.53% respectively to normal concrete beams. For geopolymer concrete beams reinforced by steel bars while the reinforcement ratio raises from 0.48% to 0.58%, the ultimate load improved by 34.25% and while the reinforcement ratio raises from 0.58% to 0.68% the ultimate load improved by 3.75%. The addition of steel or polypropylene fibers to the mix increased the failure load of GFRP-reinforced geopolymer concrete beams by 10.49% and 8.10%.

Keywords: Geopolymer concrete beams; ambient cured; GFRP bars; flexural behavior

1. Introduction

Reinforced concrete (RC) is one of the most used construction- materials worldwide. Due to environmental issues, the utility of friendly and sustainable materials in the manufacturing of reinforced concrete is currently desired and has become more popular. Geopolymer concrete is considered an innovative sustainable material that eliminates the use of cement and uses industrial by-products or commercial wastes developed with the aid of solid alumina silicates present in alkaline activator solutions [1-3]. Source materials for geopolymer concrete are fly ash, slag, metakaolin, burnt clay, and possibly blended material from the combination of the two types [3-5].

To overcome the problem of corrosion of steel reinforcement which reduces the concrete element capacity and serviceability, different types of fiber-reinforced polymer (FRP) bars have been used as reinforcement such as glass, carbon, and basalt FRP bars in addition to their benefits of high tensile stress in the direction of fibers, corrosion resistance, durability, and lower weight [6-8]. Several experimental studies used glass FRP bars as reinforcement for geopolymer concrete beams [9-11]. [12] studied the cracking of geopolymer concrete reinforced with steel and GFRP bars reinforcement and noted worse cracking resistance and faster propagation throughout the loading process for beams with FRP bars than those including steel bars.

[13, 14] studied the flexural behavior of fly ash geopolymer concrete beams reinforced with glass and carbon FRP and bars; results showed an increase in the first cracking load and ultimate load and an increase in the number of cracks and a decrease of crack width values for beams with higher reinforcement ratios. At the same reinforcement ratio, geopolymer concrete beams reinforced with CFRP bars achieved higher ultimate load and smaller crack width than beams with GFRP bars. Deflection in beams with GFRP bars was higher than that in beams with CFRP bars for the same load level, which is attributed to the lower modulus of elasticity of GFRP bars than CFRP bars. [15] investigated the flexural behavior of geopolymer concrete beams reinforced with steel fibers and showed that the increase of fiber length up to 60mm did not enhance the flexural capacity of geopolymer concrete beams due to premature fiber fracture, also geopolymer concrete beams with shorter fibers and same fiber content showed higher flexural capacity. When using hooked-end steel fibers, the flexural capacity, ductility, and cracking resistance showed significant improvement.

[16] reported that adding steel fibers to geopolymer concrete enhanced flexural strength, splitting tensile strength, ductility, load-carrying capacity, crack propagation, and post-cracking load-carrying capacity, however, it has a passive effect on workability and porosity. [17] demonstrated that geopolymer concrete beams with hybrid GFRP bars and steel bars had a greater ductile failure with lots of previous caution and with a higher number of flexural cracks that have been closely spaced in comparison to beams with GFRP bars. The flexural capacity of geopolymer concrete beams with GFRP bars decreased by 15% in comparison with beams with hybrid reinforcement of GFRP bars and steel bars.

[18] compared mechanical behavior of geopolymer concrete beams with normal concrete shows similar behavior. Additionally, Similar flexural, shear, and crack development was seen in geopolymer concrete beams with compression reinforcements of 2 Φ 8 and tension reinforcements of 2 Φ 8, 3 Φ 14, and 2 Φ 18, respectively. For the inclusion of steel fibers, equivalent values within the standard deviation were discovered for both geopolymer concrete and normal concrete. These values are much higher than those of unreinforced concretes, by a factor of more than 4 [19].

In this research work, an experimental program was conducted to investigate the flexural behavior of geopolymer concrete beams having various reinforced schemes. Most research studies of geopolymer concrete have used oven curing for specimen curing; in this study, casting and curing at room temperature to make geopolymer concrete more convenient for practical projects and encourage the usage of waste materials. The experimental program is presented in the following sections; the results are analyzed and compared with normal concrete beams.

2. EXPERIMENTAL PROGRAM

To investigate the structural behavior of geopolymer concrete beams, ten concrete beams were cast and cured at ambient temperature, then tested up to failure under four-point bending. Different reinforcement schemes were employed for the beams: steel or GFRP reinforcement bars in addition to steel and polypropylene fibers. Results of deflection, cracking, and failure load were recorded. Additionally, laboratory tests were made to determine the material properties. All the experimental works were performed in the Reinforced Concrete Laboratory of the Housing and Building National Research Center.

2.1 Materials and Mix Proportions

The mix proportions for normal and geopolymer concrete mixes employed in the experimental work are given in Table 1. The cement used was ordinary Portland cement grade I 52.50 N. Aggregate was crushed dolomite with a nominal size of 5 mm and natural siliceous sand. Superplasticizer 'Master Glenium ACE 3383' complying with EN 934-2, and ASTM C494 type A and F was added to the normal concrete mixture to enhance the workability. For preparing geopolymer concrete, the source material was ground granulated blast furnace slag which complies with ASTM C989, shown in Fig. 1(a). The physical and mechanical properties as well as the chemical analysis of slag are given in Tables 2 and 3. The alkaline activator (solution) was sodium hydroxide (NaOH) flakes, Fig. 1b, and sodium meta-silicate (Na_2SiO_3) known commercially as glass water. The fibrillated polypropylene fiber, shown in Fig. 1c, was used 0.1% by volume of concrete having the physical and mechanical properties given in Table 4.

The steel fiber used was hooked-end steel fiber with a length of 25 mm and diameter of 0.8 mm, shown in Fig. 1d. The specific gravity and tensile strength of steel fiber were 0.92 g/cm3 and 1100 N/mm2 respectively. Steel main reinforcement was high-grade steel 36/52 (deformed bars) of diameter 10 mm and 12 mm; stirrups were normal mild steel 24/35 (plain bars) of diameter 8 mm. Locally produced glass fiber reinforced bars (GFRP) of diameters 8 mm and 12 mm have the mechanical characteristics listed in Table 5. The reinforcement of beams is shown in Fig.

Fig 1. Geopolymer constituent materials and added fibers.

TABLE 1.Mix proportion for one cubic meter of concrete.

Material	Geopolymer concrete (kg/m^3)	Normal concrete (kg/m^3)
Fine aggregates (sand)	650	670
Coarse aggregates (crushed dolomite)	1150	1140
Slag	400	-
Cement	-	420
$\dfrac{Na_2SiO_3}{NaOH}$	3.0	-
Sodium silicate solution	150	-
Sodium hydroxide solution	50	-
Water content	47	165
Super Plasticizer	-	3lit

TABLE 2. Properties of ground granulated blast furnace slag.

Property		Result	Range
Specific Gravity		2.80	2.70-2.95
Density (t/m³)		1.15	1.1-1.3
Fineness	Specific Surface (cm²/g)	4088	3200-4100
	45 microns (% retained)	4.00	4-9
Insoluble Residue (%)		1.40	1-1.50
Loss of Ignition (%)		0.50	0.50-0.80

TABLE 3. Chemical analysis of Ground Granulated Blast Furnace Slag.

Component	SiO_2	Al_2O_3	CaO	MgO	Fe_2O_3	M_nO	TiO_2	Sulfide Sulfur
Percentage by weight (%)	35.40	17.40	36.87	6.83	1.40	0.35	0.11	0.24
Range (%)	32-38	14-18	32-38	6-10	0.7-1.5	0.3-0.9	0.1-0.5	0.2-0.5

TABLE 4. Physical and mechanical properties of polypropylene fibers.

Property	Value
Specific Gravity	0.91 gm/cm³
The thickness of the package	2 mm
Each fiber bandle	10
Tensile strength	370 N/mm²
Young's modulus	3750 N/mm²
Acid and salt resistance	High
Alkali resistance	Alkali proof
Electrical conductivity	Low
Melting point	160 °c
Ignition point	> 320 °c

TABLE 5. Mechanical properties of glass fiber-reinforced polymer bars.

Diameter (mm)	Ultimate tensile strength f_u(N/mm²)	Elastic Modulus E_f (kN/mm²)	Rupture strain ε_{fu}
8	416.30	34.30	0.025
12	347.50	32.67	0.05

a) Steel reinforcement　　　　　　**b)** Glass FRP reinforcement
Fig2. Schemes of reinforcement for beams.

2.2 Test Specimens Preparation

Ten specimens of concrete beams, divided into three groups, were designed and cast, as given in Table 6. All beams have a length of 2000 mm cross-section of 150 mm width and 250 mm depth. The first group of beams is reinforced with steel bars, the second and the third groups of beams are reinforced with GFRP bars, and for the last group of beams, steel fiber, and fibrillated polypropylene fiber are added by 0.5 % and 0.1 % of concrete volume respectively. Beams with steel bars had three different reinforcement ratios equal to 0.48 %, 0.58 %, and 0.68 %, also beams with GFRP bars had three different reinforcement ratios equal to 0.31 %, 0.49 %, and 0.68 %. All beams had top steel reinforcement 2 bars diameter 8 mm and stirrups 6 mm diameter at 150 mm spacing. The geometry and details of the tested beams are shown in Fig. 3. All the beams were cured at ambient temperature and stored in the laboratory, as shown in Fig. 4, until testing after 28 days after casting.
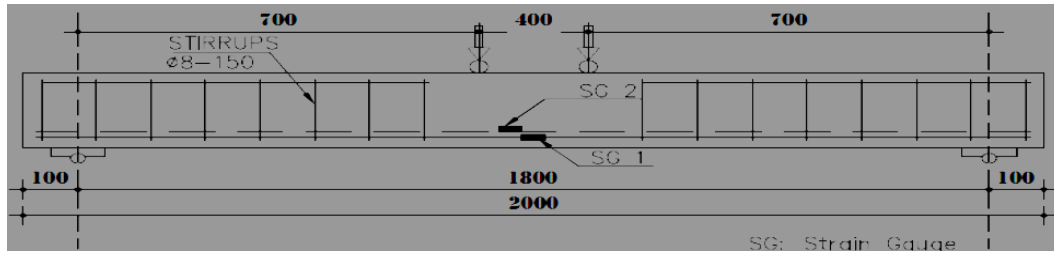
Fig3. Dimensions and reinforcement details of the tested beams.

TABLE 6. Details of the tested beams.

Group	Beam	Concrete type*	Beam dimension b(mm)	Beam dimension t(mm)	RFT. ratio (ρ) %	Bottom reinforcement Steel	Bottom reinforcement GFRP	Steel fibers %	Polypropylene Fibers %
I	B1	N	150	250	0.48	2 Φ 10	-	-	-
	B2	G	150	250	0.48	2 Φ 10	-	-	-
	B3	G	150	250	0.58	1 Φ 10 +1 Φ 12	-	-	-
	B4	G	150	250	0.68	2 Φ 12	-	-	-
II	B5	N	150	250	0.68	-	2 Φ 12	-	-
	B6	G	150	250	0.68	-	2 Φ 12	-	-
	B7	G	150	250	0.31	-	2 Φ 8	-	-
	B8	G	150	250	0.49	-	1 Φ 8 +1 Φ 12	-	-
III	B9	G	150	250	0.68	-	2 Φ 12	0.5	-
	B10	G	150	250	0.68	-	2 Φ 12	-	0.1

* N isnormal concrete, G geopolymer concrete.

Fig 4. Beam specimens after casting.

2.3 Concrete Material Tests

A 30m x 30m Cubes with dimensions 150 x 150 x 150 mm, cylinders with 150 mm diameter and 300 mm height, and prisms with dimensions 100 x100 x 500 mm were prepared for normal and geopolymer concrete mixes as shown in Fig. 5. Compressive strength and split tensile strength tests were carried out at 7 days and 28 days after the specimens' preparation and curing in accordance with ASTM C496 [20]. A flexural strength test in accordance with ASTM C 78 [21] was carried out after 28 days. Figure 6 shows the compressive strength, splitting tensile strength, and flexural strength testing apparatus. The test results are listed in Table 7.

2.4 Test Setup and Testing Procedure for Beams

All beams were tested under four-point bending using a 2000 kN capacity testing apparatus as shown in Fig. 7. To measure the deflection, three linear variable differential transformers (LVDT) were fixed on one side of each beam: at mid-span and at 400 mm distance from the right and the left end of the tested beam. Mechanical strain gauges were bonded on the bottom bars at the beam mid-span. The LVDT and strain gauges were connected to data acquisition to record their readings continuously. Cracks width was measured using a crack microscope of 0.1 mm sensitivity and the cracking pattern was recorded. The load was gradually applied in increments at a rate of approximately 4 mm/min. The cracks of the specimens were mapped and the measurements were recorded for each load increment.

Fig 5. Test specimens for normal and geopolymer concrete mixes.

Fig 6. Compressive, splitting tensile and flexural tests for concrete specimens.

TABLE 7. Compressive strength results of concrete mixes.

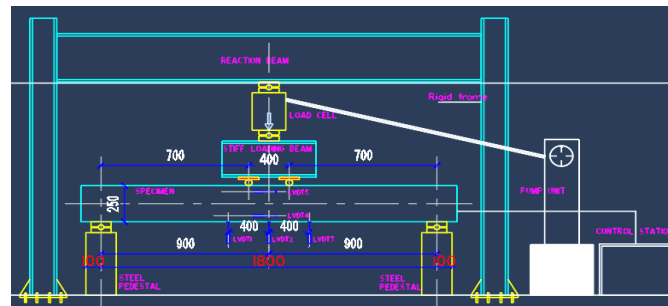| Mix	Comp. strength (N/mm²)				Splitting tens. strength (N/mm²)				Flex. strength (N/mm²)	
	7 days		28 days		7 days		28 days			
Normal Concrete	44.03	44.12	43.64	50.5	2.462	2.441	2.882	2.933	0.90	1.035
	43.51		54.43		2.716		3.176		0.975	
	44.81		53.32		2.146		2.740		1.230	
Geopolymer Concrete	45.58	44.67	55.25	53.88	3.084	2.897	2.853	3.097	2.175	2.035
	44.00		53.32		2.808		3.021		2.130	
	44.42		53.06		2.800		3.417		1.80	

Fig 7. Test set-up and instrumentation.

3. EXPERIMENTAL RESULTS AND DISCUSSION

The experimental results are given in Table 8. The initial stiffness (K), defined as the ratio between load at yield (P_y) to the corresponding mid-span deflection (δ_y), and ductility factor (DF), defined as the ratio between maximum deflection (δ_u) to the deflection at yield level (δ_y), are calculated and given in Table 9, in addition to the results of all beams compared to control beam B1. The relations between load and mid-span deflection and strain at main reinforcement bars (average of the two bars readings) for all tested beams are plotted in Figs. 8 and 9, respectively. The crack width, measured for 3 to 4 major cracks at 5kN

increment of the load is plotted in relation to the load in Fig. 10. The failure loads for all beams are plotted in Fig. 11.
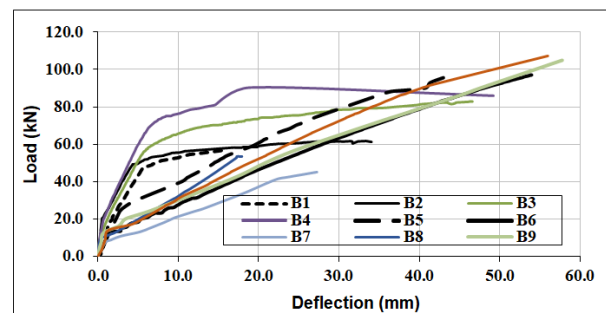

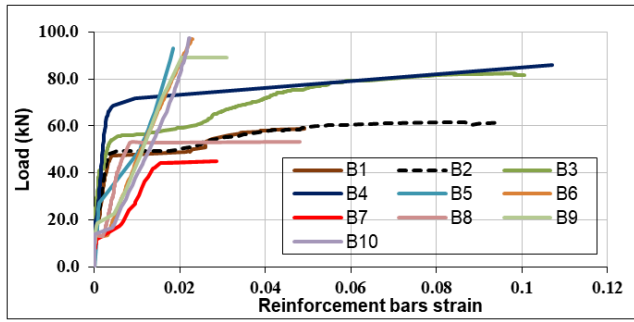**Fig 8.** Load– deflection curve of all tested beams.

Fig 9. Load - reinforcement bars strain for all beams.
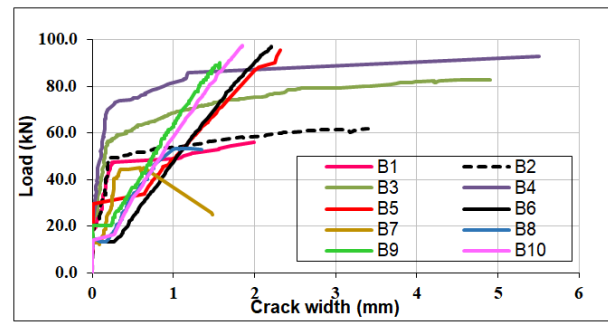

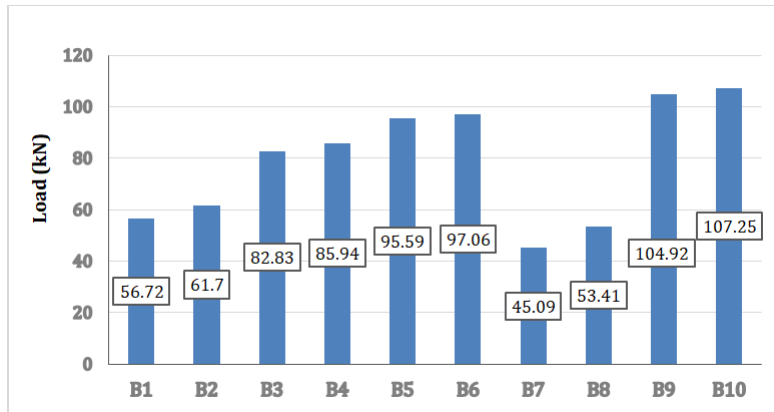**Fig 10**. Load -crack width for all beams.

Fig 11. Failure loads of all tested beams.

TABLE 8. Experimental results for the tested beams.

Group	Beam	Initial cracking load, P_{Cr} (kN)	Load at yield, P_y (kN)	Failure load, $P_{f.}$ (kN)	Max. deflection δ_u (mm)	Max. strain in bars at failure
I	B1	15.57	47.46	56.72	15.55	0.028
	B2	18.21	49.43	61.7	33.38	0.070
	B3	22.5	56.13	82.83	47.04	0.078
	B4	23.03	65.96	85.94	49.23	0.020
II	B5	19.78	29.5	95.59	43.00	0.019
	B6	13.42	22.3	97.06	53.98	0.022
	B7	11.21	14.0	45.09	27.26	0.017
	B8	12.79	20.4	53.41	17.28	0.048
III	B9	16.31	25.0	104.92	57.80	0.031
	B10	16.52	20.1	107.25	56.00	0.020

TABLE 9. Comparison of beam results with control beam

Group	Beam	Initial stiffness K (kN/mm)	Ductility factor DF	Results relative to control beams					
				$\dfrac{P_{cr}}{P_{cr}-R}$	$\dfrac{P_y}{P_y-R}$	$\dfrac{\delta_y}{\delta_y-R}$	$\dfrac{P_f}{P_{uf}-R}$	$\dfrac{K}{K_R}$	$\dfrac{DF}{DF_R}$
I	B1	8.43	2.76	1.00	1.00	1.00	1.00	1.00	1.00
	B2	10.17	6.87	1.17	1.04	0.86	1.09	1.21	2.49
	B3	9.68	8.11	1.45	1.18	1.03	1.46	1.15	2.94
	B4	11.22	8.37	1.48	1.39	1.04	1.52	1.33	3.03
II	B5	5.9	8.6	1.27	0.62	0.89	1.69	0.70	3.12
	B6	4.55	11.0	0.86	0.47	0.87	1.71	0.54	3.99
	B7	2.9	5.62	0.72	0.29	0.86	0.79	0.34	2.04
	B8	4.17	3.53	0.82	0.43	0.87	0.94	0.49	1.28
III	B9	4.9	11.33	1.05	0.56	0.91	1.85	0.58	4.11
	B10	4.06	11.31	1.06	0.42	0.88	1.90	0.48	4.10

3.1 Cracking and failure loads

By examining the results in Tables 8 and 9, it can be noticed that the initial crack load of geopolymer concrete beam B2 showed an increase of 16.89% over the normal concrete beam B1 having the same reinforcement. The first crack load for steel-reinforced geopolymer concrete beams was higher than that of GFRP-reinforced beams. On the other hand, steel-reinforced normal concrete beams showed a lower initial crack load than beams with GFRP reinforcement. The addition of steel or polypropylene fibers increased the crack and the failure loads of GFRP-reinforced geopolymer beams.

3.2 Stiffness and ductility

Compared to normal concrete beams, geopolymer beams, exhibit an enhancement in the stiffness by 21%, 15%, and 33% for beams B2, B3, and B4 with 0.48%, 0.58%, and 0.68% steel reinforcement ratios, respectively, while no significant increase in stiffness was recorded for geopolymer beams reinforced by GFRP bars, which may be explained by the low modulus of elasticity of GFRP bars. The addition of steel fibers for enhances the stiffness of beams reinforced with GFRP bars. For B9, the observed enhancement in stiffness was 122% with reference to beam B1. Moreover, For B10, the observed enhancement in stiffness was 19 %.

## 3.3 Crack patterns and failure modes

The tested beams showed initial crack at the bottom of the beam in the high bending moment region and then as the load was increased the cracks spread in the vertical direction and new cracks developed along the span with varying width and spacing of cracks. The crack patterns at failure are shown in Figs. 12, 13, and 14 for the tested beams of groups I, II, and III, respectively.

Beams for group I showed nearly the same pattern of failure and the modes of failure. The failure type was noted as a flexure failure by yielding the steel bars at nearly 70% to 85% of the failure load as mentioned before. On the stage of failure, crush in the compression zone of concrete was observed in both beams for group II and group III showed almost the same pattern of tension failure and failed due to the rapture of the GFRP bar and followed by the crushing of the concrete at the top surface under the load, due to the variance in GFRP beams reinforcement ratio.

By examining the curve representing the load and crack width relation, it can be observed that the crack width in the steel-reinforced geopolymer concrete beams is smaller than in beams reinforced by GFRP; and the reason beyond this is the higher modulus of elasticity of the steel bars than the GFRP bars. A similar result was also obtained by Ahmed et al. [13]; they noted that the geopolymer beams with lower reinforcement ratios experimented fewer amount of crack and a higher value of crack width, although several cracks and less value of crack width were noted in beams with higher reinforcement ratio.

Fig 12. Crack patterns for beams of Group I (reinforced by steel bars).
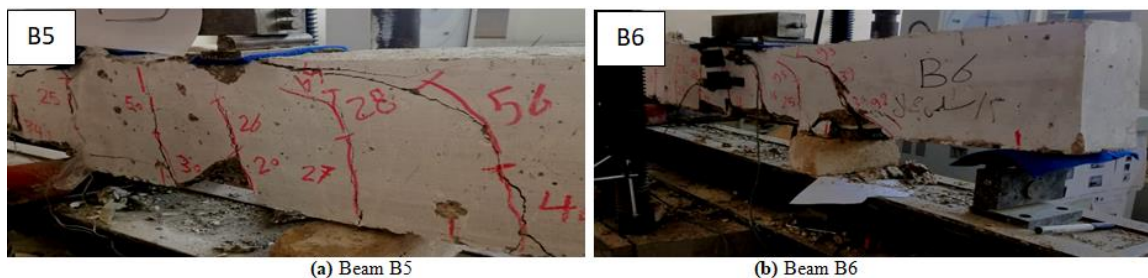
I Beam B7   (d) Beam B8
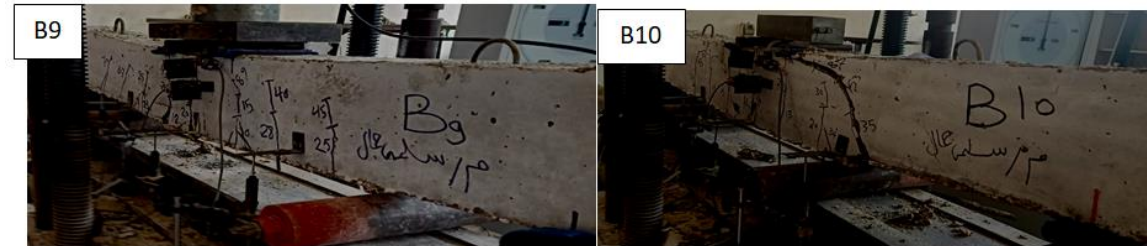**Fig 13.** Crack patterns for beams of Group II (reinforced by GFRP bars).

**Fig 14.** Crack patterns for beams of Group III (GFRP bars and fibers).

3.4 Comparison between normal and geopolymer concrete beams

The results of beams reinforced by steel bars show an increase of the initial crack load of geopolymer concrete beam B2 over the normal concrete beam B1 having the same reinforcement by16.89%, which can be attributed to the increase of tensile strength of geopolymer concrete by about 6 % than that of normal concrete. Geopolymer concrete beam has a larger failure load and larger deflection than normal concrete beam by 8.78% and 114.66 %, respectively. For GFRP-reinforced beams, geopolymer concrete beam B6 has higher failure load and deflection than normal concrete beam B5 with the same reinforcement ratio of 1.54% and 25.53 % respectively. Geopolymer concrete beam showed a smaller initial crack load by 32.15%. The strain of GFRP bars at the failure of beam B6 is 0.022 and for beam, B5 is 0.019. At load 45 kN. The crack width of beam B5 and beam B6 are 0.87 mm and 0.95 mm, respectively. The load-deflection curves of normal and geopolymer concrete beams are compared in Fig. 15.

3.5 Effect of steel reinforcement ratio for geopolymer concrete beams

For geopolymer concrete beams B2, B3, and B4 having steel reinforcement ratios of 0.48%, 0.58%, and 0.68%, respectively. The initial crack loads are 18.21, 22.5 and 23.03kN, respectively, indicating larger initial crack loads for a higher steel reinforcement ratio. Increasing the reinforcement ratio from 0.48% to 0.58% and from 0.58% to 0.68% increased the failure load by 34.25% and 3.75%, respectively. The tensile strain for steel and GFRP reinforcement bars in the geopolymer concrete beams was in the range of 0.049-0.106 and 0.022- 0.048, respectively. Variations of mid-span deflection and crack width with load are shown in Fig. 16 for the geopolymer beams reinforced by different

reinforcement ratios of steel bars. At load 45 kN the crack width of beams B2, B3 and B4 are 0.19 mm, 0.13 mm, and 0.07 mm respectively, these results show that an increase in the steel reinforcement ratio reduces the crack width. The crack patterns presented in Fig. 12 show flexural failure.
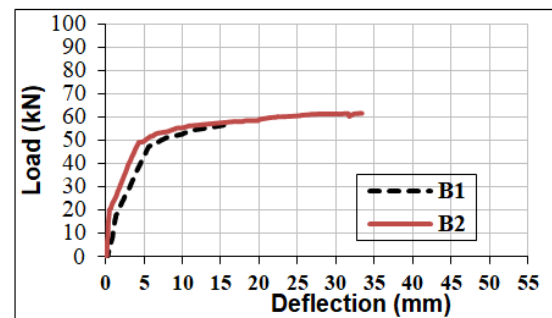
(a) Steel-reinforced beams
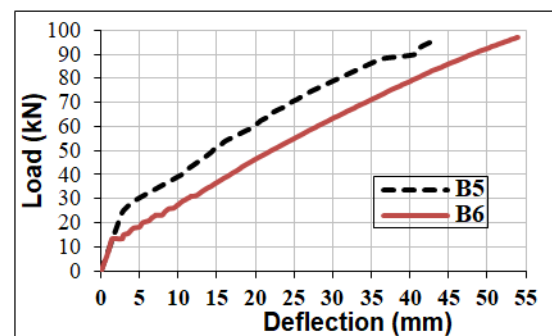
(b) GFRP-reinforced beams
Fig 15. Comparison of load-deflection curves of normal and geopolymer concrete beams.
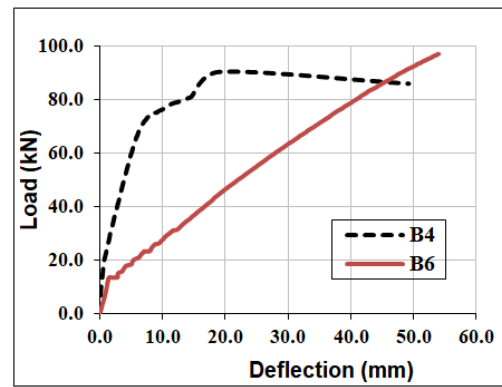
3.6 Comparison between steel and GFRP reinforcement for geopolymer concrete beams

For geopolymer concrete beam B4 reinforced by steel bars and geopolymer concrete beam B6 reinforced by

GFRP bars with the same reinforcement ratio, the experimental load-deflection and load-crack width curves are shown in Fig. 17. As shown, there is a big difference in the elastic zone between the two beams. The crack load of beam B4 is 23.03 kN and for beam, B6 is 13.42 kN, thus geopolymer concrete beam reinforced by steel bars showed a larger initial crack load. The yielding load of geopolymer concrete beam B6 reinforced by GFRP bars is 79.65% lower than that of B4 reinforced by steel bars. Beam B6 has a larger ultimate load and deflection than beam B4 by 12.94% and 9.65 %, respectively. The strain of steel bars at failure is 0.020 and for GFRP bars is 0.022. The variation of crack width with load shows that at load 45 kN, the crack width of beams B4 and B6 are 0.07 mm and 0.95 mm, respectively. The crack patterns shown in Figs. 12 and 13, indicate flexural failure.

3.7 Effect of GFRP reinforcement ratio in geopolymer concrete beams

The first crack load for GFRP-reinforced geopolymer beams was less than those with steel reinforcement. For geopolymer concrete beams B6, B7, and B8 with reinforcement ratios of 0.68%, 0.31%, and 0.49%, respectively. As the reinforcement ratio increased, the failure load increased. The increase of reinforcement ratio from 0.31% to 0.49% increased the failure load by 18.45%. The increase of reinforcement ratio from 0.31% to 0.68% caused 115.25% increase in the failure load. Comparison of the load-deflection curves for GFRP-reinforced geopolymer beams is given in Fig. 18. Crack patterns and failure modes presented in Fig. 13 show flexural failure.

(a) Load-deflection relation

(b) Load-crack width relation

Fig 16. Effect of reinforcement ratio for steel-reinforced geopolymer beams.

(a) Load−deflection relation
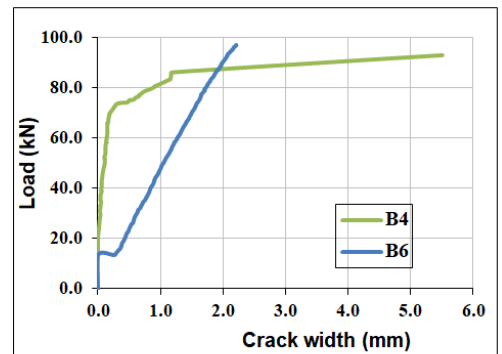
(b) Load-crack width relation

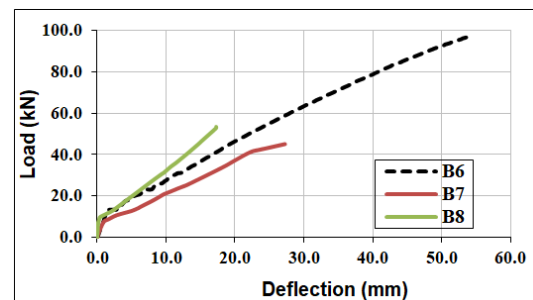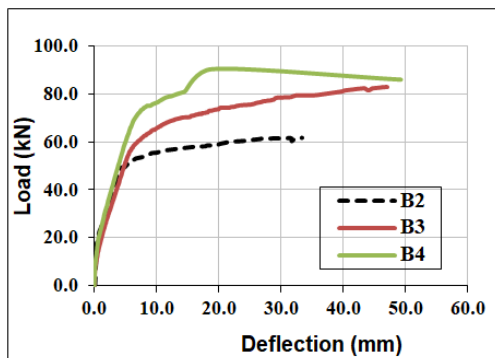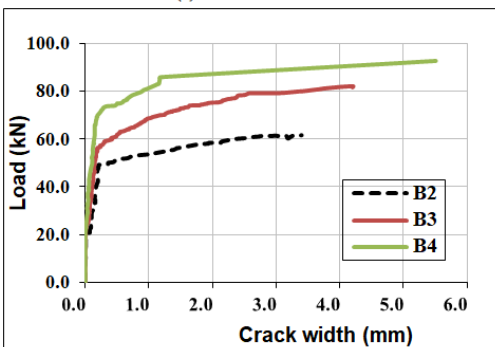Fig 17. Comparison between steel-reinforced and GFRP-reinforced geopolymer beams.

Fig 18. Effect of GFRP reinforcement ratio for geopolymer beams.

3.8 Effect of addition of steel and polypropylene fibers to GFRP-reinforced geopolymer beams

Geopolymer concrete beam B9 has the same reinforcement ratio of GFRP as B6 (bottom reinforcement of two 12 mm diameter GFRP bars) with the addition of 5% by volume steel fibers. For geopolymer beam, B10 the addition of polypropylene fibers was made as 0.1% by volume of concrete equal to 0.9 kg per cubic meter. The initial crack load of beams B6, B9, and B10 are 13.42, 16.31, and 13.86 kN, respectively; thus GFRP-reinforced geopolymer concrete beam with additional steel and polypropylene fibers showed a larger initial crack load of 21.54% and 3.3%, respectively, compared to B6. The yielding load of beam B6 is lower than beams B9 and B10 by 6.93% and 45.40%, respectively. The failure load increased by the addition of steel and polypropylene fibers by 10.49% and 8.10%, respectively, compared to beam B6. The maximum deflection of beams B9 and B10 increased by 7.08% and 3.74 %, respectively. The experimental load-

deflection and load-crack width curves are shown in Fig. 19. At load 45kN the crack width of beams B6, B9, and B10 are 0.95, 0.68, and 0.75 mm, respectively. The strain of GFRP bars at failure for beam B6, B9 and B10 are 0.022, 0.031 and 0.020, respectively. The two beams B9 and B10 have flexural failure as shown in Fig. 14.
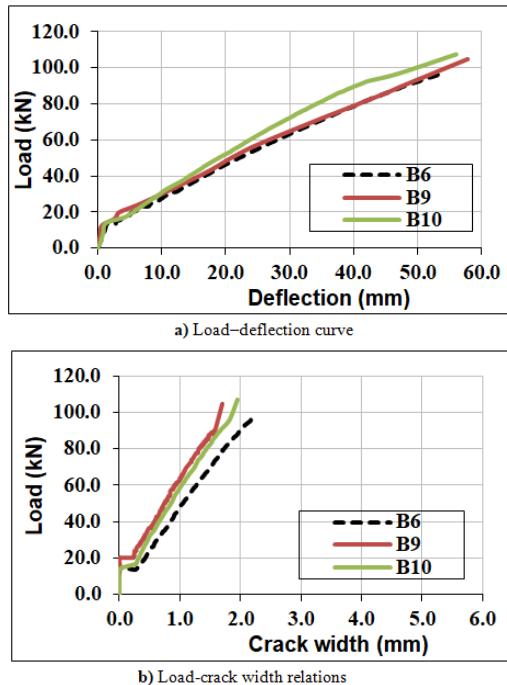

a) Load−deflection curve

b) Load-crack width relations

Fig 19. Effect of addition of steel and polypropylene fibers to GFRP geopolymer beams.

4. CONCLUSIONS

This study presented an experimental program performed on geopolymer concrete beams reinforced by several reinforcement schemes cast and cured in ambient temperature and tested under four-point bending up to failure. The experimental program, consisting of flexural testing of ten beams in addition to material testing was explained and the experimental results were discussed. The conclusions obtained from the experimental results can be summarized in the following main points:

- The findings of the study demonstrate that the production of reinforced geopolymer concrete cured at room temperature is a novel and promising strategy for reducing the consumption of cement, thereby being considered beneficial to the environment.

- The ductility of the beams was generally improved for geopolymer concrete beams compared to normal reinforced concrete beams. In addition to having a sizable capacity for inelastic deformation, it reaches its maximum strength during post-cracking deformation.

- For geopolymer concrete beams reinforced by steel bars, increasing the steel reinforcement ratio from 0.48% to 0.58% causes a 34% increase in the ultimate capacity. The ultimate capacity increase by

4% more as the reinforcement ratio increases from 0.58% to 0.68%.

- Geopolymer concrete beams exhibit an enhancement in the stiffness by 21-33%, for beams with steel reinforcement, while insignificant increase in the stiffness was recorded for beam reinforced with GFRP bars. The addition of steel fibers to the tested beams significantly improves the stiffness of the GFRP bar-reinforced beams.

- Geopolymer beams reinforced by GFRP bars showed more crack forms and larger cracks than steel-reinforced geopolymer beams. As the reinforcing GFRP ratio for the geopolymer concrete beams increase, so did the cracking width and failure load.

- Future work research work can be directed towards studying the strength as well as the serviceability and durability behavior of reinforced geopolymer concrete cured at ambient temperature reinforced by GFRP bars and dispersed fibers. Also, research should address the development of design models for reinforced geopolymer concrete elements.

Based on this investigation, consideration should be given to the feasibility and plausible future of the novel to replace normal reinforced concrete by using geopolymer reinforced concrete for repair and reinforced concrete structures.

REFERENCES

[1] C. Cheah, L. Tan, and M. Ramli, "The engineering properties and microstructure of sodium carbonate activated fly ash/slag blended mortars with silica fume," Compos Part B Eng. 160, 2019, pp. 558-572.

[2] N. Li, C. Shi, and Z. Zhang, "Understanding the roles of activators towards setting and hardening control of alkali-activated slag cement," Compos. Part B: Eng. 171, 2019, pp. 34-45.

[3] N. Li, C. Shi, Z. Zhang, H. Wang, and Y. Liu, "A review on mixture design methods for geopolymer concrete," Compos Part B Eng. 178, 2019, 107490.

[4] R. Abbas, M.A. Khereby, H.Y. Ghorab, and N. Elkhoshkhany, "Preparation of geopolymer concrete using Egyptian kaolin clay and the study of its environmental effects and economic cost," Clean Technical Environ Policy 22, 2020, pp. 669-687. doi:10.1007/s10098-020-01811-4

[5] N.S. Yacob, M.A. ElGawady, L.H. Sneed, and A. Said, "Shear strength of fly ash-based geopolymer reinforced concrete beams," Engineering Structure.196, 2019: 109298]. https://doi.org/10.1016/j.engstruct.2019.109298

[6] C. Gunasekara, D. Law, S. Bhuiyan, S. Setunge, and L. Ward, "Chloride induced corrosion in different fly ash based geopolymer concretes," Construction Building Materials 200, 2019, pp.502-513.

[7] M.H. Al-majidi, A.P. Lampropoulos, A.B. Cundy, O.T. Tsioulou and S. Alrekabi, "Flexural performance of reinforced concrete beams strengthened with fiber reinforced geopolymer concrete under accelerated corrosion," Structures 19, 2019; pp. 394-410. doi:10.1016/j.istruc.2019.02.005

[8] 8. R. Alzeebaree, A. Çevik, B. Nematollahi, J. Sanjayan, A. Mohammedameen, and M.E. Gülşan, "Mechanical properties and durability of unconfined and confined geopolymer concrete with fiber reinforced polymers exposed to sulfuric acid," Construction Building Materials. 215, 2019, pp. 15-32.

[9] G.B. Maranan, A.C. Manalo, B. Benmokrane, W. Karunasena, P. Mendis and T.Q. Nguyen, "Shear behavior of geopolymer-concrete beams transversely reinforced with continuous rectangular GFRP composite spirals," Composite Structure 187, 2018, pp.454-465. doi:10.1016/j.compstruct.2017.12.080

[10] 10. G.B. Maranan, A.C. Manalo, B. Benmokrane, W. Karunasena, and P. Mendis, "Evaluation of the flexural strength and serviceability of geopolymer concrete beams reinforced with glass-fiber-reinforced polymer (GFRP) bars," Eng. Struct.101, 2015, pp. 529-541. doi:10.1016/j.engstruct.2015.08.003

[11] J. Goonewardena, K. Ghabraie, and M. Subhani, "Flexural performance of FRP-reinforced geopolymer concrete beam," Journal of Composite Science. 4(4), 2020. doi:10.3390/jcs4040187

[12] K. Rashid, X. Li, Y. Xie, J. Deng and F. Zhang. "Cracking behavior of geopolymer concrete beams reinforced with steel and fiber reinforced polymer bars under flexural load," Composite Part B: Eng. 186, 2020: 107777. doi:10.1016/j.compositesb.2020.107777

[13] H.Q. Ahmed, D.K. Jaf and S.A. Yaseen, "Comparison of the flexural performance and behavior of fly-ash-based geopolymer concrete beams reinforced with CFRP and GFRP bars," Adv Mat Sc Eng., 2020:3495276. doi.org/10.1155/2020/3495276.

[14] H.Q. Ahmed, D.K. Jaf and S.A. Yaseen, "Flexural strength and failure of geopolymer concrete beams reinforced with carbon fiber-reinforced polymer bars," Construction Build Mater. 231, 2020:117185. doi:10.1016/j.conbuildmat.2019.117185

[15] T.T.Tran, T.M. Pham and H. Hao, "Experimental and analytical investigation on flexural behavior of ambient cured geopolymer concrete beams reinforced with steel fibers," Eng. Struct. 200, 2019:109707. doi:10.1016/j.engstruct.2019.109707

[16] A.M. Rashad, "Effect of steel fibers on geopolymer properties – The best synopsis for civil engineer," Construction Build Mater. 246, 2020:118534. doi:10.1016/j.conbuildmat.2020.118534

[17] G.B. Maranan, A.C. Manalo, B. Benmokrane, W. Karunasena, P. Mendis and T.Q. Nguyen, "Flexural behavior of geopolymer-concrete beams longitudinally reinforced with GFRP and steel hybrid reinforcements," Eng. Struct. 182, 2019, pp.141-152. doi:10.1016/j.engstruct.2018.12.073

[18] I. C. Ali, O. Ahmet, S.Ahmet, and C. A.Mehmet, "Numerical analysis of flexural and shear behaviors of geopolymer concrete beams," Journal of Sustainable Construction Materials and Technologies, Vol. 7, Issue. 2, pp. 70–80, June 2022.

[19] Bianca M. A., Mathaus M. L., Veronica S. C., Kamila S. P., Michelle S. O., Afonso R. G., and Sergio N. M., "Fatigue behavior of steel fiber reinforced geopolymer concrete Alisson Clay Rios da Silva," Case Studies in Construction Materials. 16, 2022, e00829.

[20] ASTM Standard C 496/C 496 M-11-04, (2004),"Standard Test Method for Splitting Tensile Strength of Cylindrical Concrete Specimens", West Conshohocken, PA, USA.

[21] ASTM Standard C 78 /C 78-M-10-02, (2002), "Standard Test Method for Flexural Strength of Concrete (Using Simple Beam with Third-Point Loading) ", West Conshohocken, PA, USA.Doljak, Dejan, Stanojevic´ , Gorica, 2017. Evaluation of natural conditions for site selection of ground-mounted photovoltaic power plants in Serbia. Energy 127, 291–300. https://doi.org/10.1016/j.energy.2017.03.140.